

Comparisons of BCS Nuclear Wave Functions with Exact Solutions

M. RHO* AND J. O. RASMUSSEN

Lawrence Radiation Laboratory, University of California, Berkeley, California

(Received 27 April 1964)

The validity of the Bardeen-Cooper-Schrieffer variational method is re-examined for two nuclear-model cases, one resembling the system of deformed nuclei and the other spherical nuclei. For simplicity, a constant-pairing-force approximation is adopted. The projected BCS wave functions compare badly with the exact wave functions at pairing-force strength around the critical force strength, and only for sufficiently strong pairing forces does the BCS method seem to approach the exact. For the spherical case, the average value of the pair operator ($\frac{1}{2}N$) is also calculated over a wide range of force strength, and the general behavior is found to be consistent with the results obtained on the wave-function components. The errors in eigenvalues are computed, and discussions are given as to the possible sources of the deviations.

I. INTRODUCTION

THERE has been a considerable amount of work devoted to the examination of the superconductivity theory of Bardeen, Cooper, and Schrieffer (BCS),¹ and of Bogoliubov² applied to nuclear structure problems. The BCS variational approach (or equivalently Bogoliubov lowest order "compensation" method) seems the best for larger pairing-force strength and larger number of particles. It is well known that the ordinary BCS wave functions fail to conserve the number of particles. Attention has been given to the improved wave functions obtained by taking only those components of the BCS wave function which conserve the particle number.³ There is generally a lowering in eigenvalue accompanying the projection procedure.

We will be mainly concerned here with an examination of the errors remaining after projecting the proper particle number components from the lowest BCS solutions of some simple systems. Comparison is made with exact solutions over a wide range of pairing-force strength. We use only a simple constant pairing-force Hamiltonian and do not consider higher order corrections to BCS solutions such as admixture of 4-quasi-particle components.

First, we examine a half-filled system with the nucleon pairs in six equally spaced levels. Such a system has some similarity to those in deformed nuclei. Second, we study in greater detail the case of two orbitals with the same pair degeneracy Ω , and with Ω pairs of nucleons. In particular, we study the case of $\Omega=5$ (we call this a "symmetric case"). We shall also examine an unsymmetric case where $\Omega_u \neq \Omega_l$. For example, $\Omega_u=3$, $\Omega_l=4$, with four pairs of nucleons.

These systems all have in common the feature that below a certain critical pairing-force strength there is

no nontrivial BCS solution. That is, at low force strength, the BCS approximation gives no configuration mixing whatsoever, obviously a serious defect. From simple perturbation theory it is clear that no matter how small the residual force is, there will always be some configuration mixing. This spurious "threshold" behavior is not exhibited by BCS solutions for systems where a partly filled degenerate level lies at the Fermi surface. Thus the well-studied system of a single, partly filled degenerate orbital does not exhibit this "threshold" behavior.⁴

II. A REVIEW OF BCS SOLUTIONS

This section is intended to define the notation.⁵ Let us take the convention of writing a complete set of quantum numbers by Greek letters, and all except the magnetic quantum number by Roman letters, i.e., $\alpha = (\eta_a l_a j_a m_a \dots)$, and $a = (\eta_a l_a j_a \dots)$. In this notation, the BCS reduced Hamiltonian is given by (for constant force strength)

$$H_{\text{red}} = \sum_{\alpha} \epsilon_{\alpha} a_{\alpha}^{\dagger} a_{\alpha} - (G/4) \sum_{\alpha\beta} a_{\alpha}^{\dagger} a_{-\alpha}^{\dagger} a_{-\beta} a_{\beta}, \quad (1)$$

where the fermion operator a_{α} satisfies the usual anticommutation rule. Notice that this Hamiltonian describes only the scattering of pairs of particles in time-reversed pair states. An obvious generalization would be to replace the interaction term by $(G/4) \sum_{\alpha\beta\gamma\delta} a_{\alpha}^{\dagger} a_{\beta}^{\dagger} a_{\gamma} a_{\delta}$. Using the trial wave function

$$\Psi_0 = \sum_{\alpha} (u_{\alpha} + v_{\alpha} a_{\alpha}^{\dagger} a_{-\alpha}^{\dagger}) |0\rangle,$$

and taking the expectation value of Eq. (1), a variation with respect to v_{α} gives

$$2(\epsilon_{\alpha} - \lambda) u_{\alpha} v_{\alpha} - G \sum_{\beta} u_{\beta} v_{\beta} (u_{\alpha}^2 - v_{\alpha}^2) - 2G v_{\alpha}^2 u_{\alpha} v_{\alpha} = 0. \quad (2)$$

Following the usual procedure,⁶ we drop the last term.

⁴ B. R. Mottelson, in *The Many Body Problem* (Dunod Cie., Paris, 1959).

⁵ See for an extensive discussion, S. T. Belyaev, *Kgl. Danske Videnskab. Selskab, Mat. Fys. Medd.* **31**, No. 11 (1959).

⁶ For example, S. G. Nilsson and O. Prior, *Kgl. Danske Videnskab. Selskab, Mat. Fys. Medd.* **32**, No. 16 (1960).

* Present address: Service de Physique Théorique, Centre d'Etudes Nucléaires de Saclay, Gif-sur-Yvette, France.

¹ J. Bardeen, L. N. Cooper, and J. R. Schrieffer, *Phys. Rev.* **108**, 1175 (1959).

² N. N. Bogoliubov, *Nuovo Cimento* **7**, 794 (1958); J. G. Valatin, *ibid.* **7**, 843 (1958).

³ See for example, B. F. Bayman, *Nucl. Phys.* **15**, 33 (1960); A. K. Kerman, R. D. Lawson, and M. H. Macfarlane, *Phys. Rev.* **124**, 162 (1961); K. Dietrich, H. J. Mang, and J. Pradal, *Phys. Rev.* **135**, B22 (1964).

Then we obtain

$$\frac{1}{2}G \sum_{\alpha>0} \frac{1}{[(\epsilon_\alpha - \lambda)^2 + \Delta^2]^{1/2}} = 1, \quad (3)$$

$$\Delta = G \sum_{\alpha>0} u_\alpha v_\alpha, \quad (4)$$

$$\begin{pmatrix} v_\alpha^2 \\ u_\alpha^2 \end{pmatrix} = \frac{1}{2} \left[1 \mp \frac{\epsilon_\alpha - \lambda}{[(\epsilon_\alpha - \lambda)^2 + \Delta^2]^{1/2}} \right], \quad (5)$$

with

$$N = \sum_\alpha n_\alpha = 2 \sum_{\alpha>0} v_\alpha^2 = \sum_{\alpha>0} \left\{ 1 - \frac{\epsilon_\alpha - \lambda}{[(\epsilon_\alpha - \lambda)^2 + \Delta^2]^{1/2}} \right\}. \quad (6)$$

In spherical representation, the summation index $\alpha (>0)$ is replaced by a Roman index, while multiplying the summand by $\Omega_\alpha = j_\alpha + \frac{1}{2}$. All the subscripts should then be in Roman letters.

The nonlinear equation (3) with Eqs. (4), (5), and (6) can be solved analytically only for exceptional cases (an example is given later); however, iterative solutions can be easily obtained by an electronic computer for more general cases.

III. UNIFORM SPACING (6-LEVEL) CASE

We consider here a system with three pairs of nucleons in six doubly degenerate levels; this is a case rather similar to those in deformed nuclei. The BCS

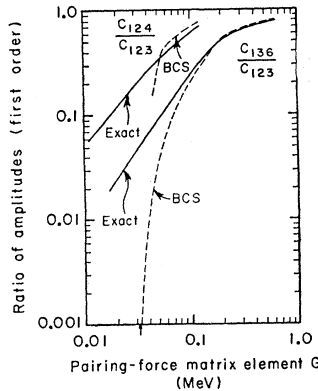


FIG. 1. The ratios of amplitudes, C_{124}/C_{123} and C_{136}/C_{123} in the six-level, three-pair nondegenerate model with $\epsilon = 100$ keV. The arrow indicates the critical force strength.

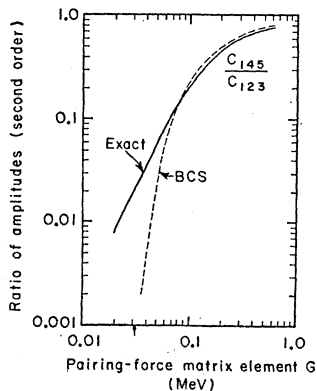


FIG. 2. The ratio of amplitudes (2nd order) C_{145}/C_{123} in the six-level three-pair nondegenerate model with $\epsilon = 100$ keV.

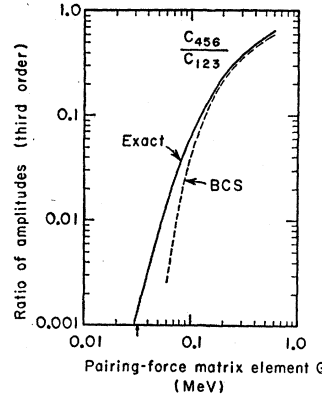


FIG. 3. The ratio of amplitudes (3rd order) C_{456}/C_{123} in the six-level, three-pair nondegenerate model with $\epsilon = 100$ keV.

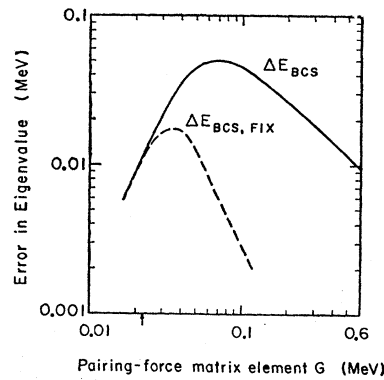


FIG. 4. Error in eigenvalues for the ordinary and projected BCS solutions of the six-level, three-pair model as deduced by comparison with exact solutions of 20×20 matrix.

equations then yield six independent parameters v_α 's. The exact solution, which amounts to diagonalizing the reduced Hamiltonian (1) exactly, has twenty components. The wave function then has the form

$$\Psi_{ex} = \sum_{\alpha\beta\gamma} C_{\alpha\beta\gamma} A_{\alpha\beta\gamma}^+ |0\rangle, \quad (7)$$

with $A_{\alpha\beta\gamma}^+ = a_\alpha^+ a_{-\alpha}^+ a_\beta^+ a_{-\beta}^+ a_\gamma^+ a_{-\gamma}^+$. If we label the levels as 1, 2, ..., 6 in increasing order, then C_{123} is the amplitude for occupation of levels 1, 2, 3, C_{124} is the amplitude with one pair excited and so on.

In order to compare the amplitude (7) with the BCS wave function (Ψ), we need to project the appropriate components from the BCS wave function. The remaining parts in the BCS wave function are spurious, but necessary to make the wave function easy to handle. Defining a projection operator by

$$P(\mu\nu\epsilon)\Psi_0 = \left(\prod_{\lambda \neq \mu, \nu, \epsilon} u_\lambda \right) v_\mu v_\nu v_\epsilon A_{\mu\nu\epsilon}^+ |0\rangle, \quad (8)$$

we have

$$\frac{\langle 0 | A_{124} P(124) | \Psi_0 \rangle}{\langle 0 | A_{123} P(123) | \Psi_0 \rangle} = \frac{v_1 v_2 u_3 v_4 u_5 u_6}{v_1 v_2 v_3 u_4 u_5 u_6} = \frac{u_3 v_4}{v_3 u_4}, \quad (9)$$

which may be compared with C_{124}/C_{123} of the exact solution.

In Figs. 1 through 3 are given the ratios of amplitudes for both the BCS and exact solutions. We have

taken six equally spaced levels each separated by 100 keV. Figure 1 shows the comparison for two of the nine amplitudes that involve a single pair promotion from the lowest levels 1, 2, 3 across the Fermi energy to 4, 5, or 6. The limiting slope in the weak-force limit is unity, corresponding to the first power dependence on G from first-order perturbation theory. For the ratio C_{124}/C_{123} the BCS value crosses the exact for a force strength just above critical. For the other ratio plotted, the BCS ratio only very slightly ever exceeds the exact. The second-order amplitudes plotted in Fig. 2 do not cross until about three times critical force strength, while for the third order amplitude of Fig. 3 the BCS always lies below the exact.

In Fig. 4 are plotted the errors in eigenvalues of ordinary and projected BCS solutions of the system in question, as deduced by comparison with exact solutions of the 20×20 matrix. Notice that the curves are superimposed up to the critical force strength and thereafter the projected solution shows much less error. The maximum error for the projected solution comes at a force less than twice critical strength, and this error is about 17 keV, or one-sixth the single-particle level spacing of 100 keV. The ordinary BCS eigenvalue may show an error of as much as half the single-particle level spacing.

IV. SYMMETRIC TWO-DEGENERATE-LEVEL CASE

In this section, we examine the case of Ω pairs of nucleons in two levels of pair degeneracy Ω , separated by an energy difference of ϵ . In this case, the BCS equation can be solved analytically, and interesting features emerge from the comparison of the BCS and exact solutions. In order to be more general, a parallel calculation with two levels of different degeneracy ($\Omega_l=4$, $\Omega_\mu=3$, $N=8$) is also performed. In the latter case, no such simple analytical BCS solution is available, and hence the solutions are obtained by iterative numerical solution of the Belyaev equations.

What we will examine here are the following: First we calculate $\langle \frac{1}{2}N \rangle$ for the upper level and compare the BCS and exact wave functions, and second we compare the ratios of amplitudes in a manner analogous to Sec. III.

A. Quasispin Method

For the system with large magnetic degeneracy, the Hamiltonian (1) can be easily diagonalized by the spin-wave method introduced by Anderson,⁷ and later applied to nuclear problem by Kerman *et al.*⁸ Let us use this method to calculate explicitly the Hamiltonian matrix of the system.

Following Kerman *et al.*, we introduce the quasispin

operators

$$\begin{aligned} \mathfrak{S}_+ &= \sum_a S_+(a) = \sum_{\alpha>0} a_\alpha^+ a_{-\alpha}^+, \\ \mathfrak{S}_- &= \sum_a S_-(a) = \sum_{\alpha>0} a_{-\alpha} a_\alpha, \end{aligned} \quad (10)$$

$$\begin{aligned} \mathfrak{S}_z &= \frac{1}{2} \sum_{\alpha>0} \{a_\alpha^+ a_\alpha - a_{-\alpha} a_{-\alpha}^+\} \\ &= \sum_a S_z(a) = \frac{1}{2} \sum_\alpha a_\alpha^+ a_\alpha - \frac{1}{2} \sum_\alpha \Omega(a), \end{aligned}$$

where $\Omega(a) = j_a + \frac{1}{2}$, and $\alpha > 0$ restricts the summation over only positive magnetic quantum numbers $\sum_{\alpha>0} = \sum_{a, m_a > 0}$ while α goes over both positive and negative values. In the operators of (10), we have for (1)

$$H_{\text{red}} = 2 \sum_a \epsilon_a S_z(a) + \sum_a \epsilon_a \Omega(a) - G \mathfrak{S}_+ \mathfrak{S}_-. \quad (11)$$

In the strong-coupling limit ($G/\bar{\epsilon} \gg 1$, where $\bar{\epsilon}$ is an average level spacing)

$$H_{\text{red}}^S \approx -G \mathfrak{S}_+ \mathfrak{S}_-, \quad (12a)$$

and in the weak-coupling limit, only the kinetic energy term remains

$$H_{\text{red}}^W \approx 2 \sum_a \epsilon_a [S_z(a) + \Omega(a)/2]. \quad (12b)$$

Thus, one could take a state that is diagonal in either H_{red}^W or H_{red}^S for a zero-order wave function. We introduce quasispin quantum numbers as follows: With a configuration given by

$$[a^{n_1} b^{n_2} c^{n_3} \dots], \quad (13)$$

the quasispin parameters are fixed thus

$$\begin{aligned} \sigma_\kappa &= \max |n_\kappa - \Omega_\kappa| / 2, \\ \sigma_\kappa^0 &= (n_\kappa - \Omega_\kappa) / 2, \\ \sigma &= \sum_\kappa \Omega_\kappa / 2, \\ \sigma_0 &= \sum_\kappa (n_\kappa - \Omega_\kappa) / 2, \\ \kappa &= a, b, \dots, \end{aligned}$$

which yield basis vectors of form

$$|\sigma_a \sigma_a^0, \sigma_b \sigma_b^0, \dots\rangle. \quad (14)$$

The seniority quantum number is related to the quantity given above by

$$\nu_a = \Omega_a - 2\sigma_a.$$

Thus the ground state of even-particle system is given by

$$\sigma_a = \frac{1}{2} \Omega_a,$$

which implies that we have to construct the wave functions with $\sigma_a = \frac{1}{2} \Omega_a$. Thus an empty orbital is

⁷ P. W. Anderson, Phys. Rev. **112**, 1900 (1958).

⁸ See Kerman *et al.*, Ref. 3.

denoted by $|\frac{1}{2}\Omega_a, -\frac{1}{2}\Omega_a\rangle$, and hence a state with p pairs in a may be generated by

$$(S_+(a))^p |\frac{1}{2}\Omega_a, -\frac{1}{2}\Omega_a\rangle, \\ = \{p! \Omega_a (\Omega_a - 1) \cdots (\Omega_a - p + 1)\}^{1/2} \\ \times |\frac{1}{2}\Omega_a, -\frac{1}{2}\Omega_a + p\rangle. \quad (15)$$

We have the usual relations for angular momentum operations:

$$S_z(a) |\sigma_1 \sigma_1^0; \cdots; \sigma_a \sigma_a^0, \cdots\rangle \\ = \sigma_a^0 |\sigma_1 \sigma_1^0; \cdots; \sigma_a \sigma_a^0, \cdots\rangle, \quad (16)$$

$$S^2(a) |\sigma_1 \sigma_1^0; \cdots; \sigma_a \sigma_a^0, \cdots\rangle \\ = \sigma_a (\sigma_a + 1) |\sigma_1 \sigma_1^0; \cdots; \sigma_a \sigma_a^0, \cdots\rangle, \quad (17)$$

$$S_{\pm}(a) |\sigma_1 \sigma_1^0; \cdots; \sigma_a \sigma_a^0\rangle = \{\sigma_a (\sigma_a + 1) - \sigma_a^0 (\sigma_a^0 \pm 1)\}^{1/2} \\ \times |\sigma_1 \sigma_1^0; \cdots; \sigma_a \sigma_a^0 \pm 1, \cdots\rangle. \quad (18)$$

One might couple the σ_i values by twos to resultant vectors,⁹ but for our purpose it is more convenient to choose the m representation. Now a matrix element of the Hamiltonian given by Eq. (11) can be easily

written down. Let us specialize for two Ω -fold degenerate levels. The matrix elements are as follows:

$$\langle \sigma_1 \sigma_1^0, \sigma_2 \sigma_2^0 | H_{\text{red}} | \sigma_1 \sigma_1^{0'}, \sigma_2 \sigma_2^{0'} \rangle \\ = 2[\epsilon_1 (\sigma_1^0 + \frac{1}{2}\Omega_1) + \epsilon_2 (\sigma_2^0 + \frac{1}{2}\Omega_2)] \delta(\sigma_1^0 \sigma_1^{0'}) \delta(\sigma_2^0 \sigma_2^{0'}) \\ - G \delta(\sigma_1^0 \sigma_1^{0'}) \delta(\sigma_2^0 \sigma_2^{0'}) \{[\sigma_1 (\sigma_1 + 1) - \sigma_1^0 (\sigma_1^0 - 1)] \\ + [\sigma_2 (\sigma_2 + 1) - \sigma_2^0 (\sigma_2^0 - 1)]\} \\ - G \delta(\sigma_1^{0'} \sigma_1^0 \pm 1) \delta(\sigma_2^{0'} \sigma_2^0 \mp 1) \{[\sigma_1 (\sigma_1 + 1) \\ - \sigma_1^0 (\sigma_1^0 \pm 1)]^{1/2} + [\sigma_2 (\sigma_2 + 1) - \sigma_2^0 (\sigma_2^0 \mp 1)]^{1/2}\}. \quad (19)$$

In the coupled representation (i.e., in the representation where $S_+ S_-$ is diagonal), the last two terms may be written as

$$\langle \sigma_1 \sigma_1^0, \sigma_2 \sigma_2^0 | S_+ S_- | \sigma_1 \sigma_1^{0'}, \sigma_2 \sigma_2^{0'} \rangle \\ = \sum_{\sigma} C(\sigma_1 \sigma_2 \sigma; \sigma_1^0 \sigma_2^0 \sigma_0) C(\sigma_1 \sigma_2 \sigma; \sigma_1^{0'} \sigma_2^{0'} \sigma_0) \\ \times [\sigma (\sigma + 1) - \sigma_0 (\sigma_0 - 1)], \quad (20)$$

where $C(\cdots)$ is the usual Clebsch-Gordan coefficient.

If we put $\Omega_a = \Omega_b = 5$, $N = 10$, $\epsilon_a - \epsilon_b \equiv \epsilon$ in the "symmetric" example we get a matrix of the form

$$H_{\text{red}} = \begin{pmatrix} -5G & -5G & 0 & 0 & 0 & 0 \\ -5G & 2\epsilon - 13G & -8G & 0 & 0 & 0 \\ 0 & -8G & 4\epsilon - 17G & -9G & 0 & 0 \\ 0 & 0 & -9G & 6\epsilon - 17G & -8G & 0 \\ 0 & 0 & 0 & -8G & 8\epsilon - 13G & -5G \\ 0 & 0 & 0 & 0 & -5G & 10\epsilon - 5G \end{pmatrix}. \quad (21)$$

For a slightly "nonsymmetric" case with $\Omega_a = 4$, $\Omega_b = 3$, $N = 8$, we have

$$H_{\text{red}} = \begin{pmatrix} -4G & -2\sqrt{3}G & 0 & 0 \\ -2\sqrt{3}G & 2\epsilon - 9G & -2\sqrt{6}G & 0 \\ 0 & -2\sqrt{6}G & 4\epsilon - 10G & -3\sqrt{2}G \\ 0 & 0 & -3\sqrt{2}G & 6\epsilon - 7G \end{pmatrix}. \quad (22)$$

Let us consider the behavior at large and small G of the lowest state eigenfunction of the symmetric problem. For small G (i.e., $G/\epsilon \ll 1$), we get by first-order perturbation theory for the average number of pairs $\langle \frac{1}{2}N_u \rangle$ excited to the upper level,

$$\lim_{G \rightarrow 0} \langle \frac{1}{2}N_u \rangle \approx 25G^2 / (2\epsilon - 8G)^2, \quad (23)$$

where $\epsilon_u - \epsilon_l = \epsilon$, the subscripts l , and u denoting lower and upper levels, respectively. The ratio of amplitudes C_1/C_0 (where the subscript denotes the number of pairs excited) behaves like $5G/2(\epsilon - 4G)$ for low G values.

In the strong-pairing-force limit ($G/\epsilon \gg 1$)

$$\lim_{G \rightarrow \infty} \langle \frac{1}{2}N_u \rangle = \frac{1}{2}\Omega. \quad (24)$$

As we shall see later, this high- G limit coincides with the BCS method.

⁹ A. de-Shalit and I. Talmi, *Nuclear Shell Theory* (Academic Press Inc., New York, 1963).

B. The BCS Solutions

In the case where $\Omega_l = \Omega_u = \Omega$ and the number of particles makes the system half-filled, the chemical potential λ lies exactly half-way between upper and lower levels. If we measure the single-particle energy from $\lambda = 0$, obviously $-\epsilon_l = \epsilon_u = \frac{1}{2}\epsilon$. Therefore, the solutions of the set of BCS equations are readily obtained. Dropping the last term in Eq. (2), we have

$$u_l^2 = v_u^2 = u_l v_u = \left(1 - \frac{\epsilon}{2G\Omega}\right) / 2, \\ u_u^2 = v_l^2 = u_u v_l = \left(1 + \frac{\epsilon}{2G\Omega}\right) / 2, \quad (25)$$

$$\Delta^2 = (G\Omega)^2 - \frac{1}{4}\epsilon^2.$$

From Eq. (25), we see that in order for Δ to be real, the condition should hold

$$G \geq \epsilon/2\Omega. \quad (26)$$

Thus, the BCS solution breaks down for pairing force smaller than $\epsilon/2\Omega$. It is instructive to notice that the "critical" pairing-force strength given by $G_c = \epsilon/2\Omega$ is proportional to ϵ/Ω ; thus, the requirement that ϵ/Ω should be small for the validity of BCS solutions is in fact related to the size of G_c .

Using Eq. (25), we obtain

$$\langle \frac{1}{2}N_u \rangle = \Omega v_u^2 = \frac{1}{2}\Omega[1 - (\epsilon/2G\Omega)]. \quad (27)$$

Thus the behavior of the BCS solution at small pairing-force strength is drastically different from the exact solution. One can see that the BCS value of $\langle \frac{1}{2}N_u \rangle$ falls much faster than the exact value for small G .

As was mentioned before, as G becomes large, $\langle \frac{1}{2}N_u \rangle$ approaches $\frac{1}{2}\Omega$, and the BCS and exact solutions approach each other at large force strength G .

For the purpose of comparing the amplitudes, a slightly different representation of the BCS wave function is needed. The BCS wave function, Ψ_0 , has to be rewritten in the quasispin operators introduced in Eq. (10), since the exact wave function is expanded in the basis vectors of the type

$$|a^{2p}\rangle \equiv |\frac{1}{2}\Omega_a, -\frac{1}{2}\Omega_a + p\rangle \\ = [p! \Omega_a (\Omega_a - 1) \cdots (\Omega_a - p + 1)]^{-1/2} (S_+(a))^p |0_a\rangle, \quad (28)$$

where

$$|0_a\rangle = |\frac{1}{2}\Omega_a, -\frac{1}{2}\Omega_a\rangle$$

denotes an empty a orbital, and p denotes the number of pairs in the a shell. A rather straightforward manipulation of Ψ_0 easily gives

$$\Psi_0 = \prod_{\kappa=a, b, \dots} u_{\kappa}^{\Omega_{\kappa}} \left[\sum_{\lambda=0}^{\Omega_{\kappa}} \frac{1}{\lambda!} \left(\frac{v_{\kappa}}{u_{\kappa}}\right)^{\lambda} (S_+(\kappa))^{\lambda} |0_{\kappa}\rangle \right]. \quad (29)$$

In the representation of Eq. (28),

$$\Psi_0 = \prod_{\kappa=a, b, \dots} u_{\kappa}^{\Omega_{\kappa}} \left[|k^0\rangle + \sum_{\lambda=1}^{\Omega_{\kappa}} \sqrt{\lambda!} \left(\frac{v_{\kappa}}{u_{\kappa}}\right)^{\lambda} \binom{\Omega_{\kappa}}{\lambda} |k^{2\lambda}\rangle \right], \quad (30)$$

where we have used the usual binomial-coefficient notation $\binom{n}{m} = \frac{n!}{(n-m)!m!}$. Now we designate the amplitude of the lowest zero-order configuration by C_0 , the next by C_1 , and so on. In the absence of interaction, the lowest configuration with p pairs is then $|a^p b^0 c^0 \dots\rangle$, where a is the lowest j shell, the next $|a^{p-2} b^2 c^0 \dots\rangle$ a state with a pair excited from a to b .

From Eq. (30), we have (for the case of $P = \Omega_a$)

$$C_0 = v_a^{\Omega_a} \prod_{\kappa=b, c, \dots} u_{\kappa}^{\Omega_{\kappa}}, \quad (31) \\ C_1 = \Omega_a \Omega_b u_a^{\Omega_a - 1} v_a u_b v_b^{\Omega_b - 1} \prod_{\kappa=c, d, \dots} u_{\kappa}^{\Omega_{\kappa}}, \text{ etc.}$$

If we specialize with the symmetric two-level case, the result becomes simple. Letting $\Omega_a = \Omega_b = \Omega$, and $P_a + P_b = \Omega$ ($P_a + P_b$ is the total number of pairs).

$$C_0 \equiv C[a^{2\Omega}] = (v_a u_b)^{\Omega}, \\ C_1 \equiv C[a^{2\Omega-2} b^2] = \Omega u_a v_a^{\Omega-1} u_b^{\Omega-1} v_b, \\ C_2 \equiv C[a^{2\Omega-4} b^4] = \frac{1}{2} \Omega (\Omega - 1) u_a^2 v_a^{\Omega-2} u_b^{\Omega-2} v_b^2, \quad (32) \\ \vdots \\ C_p \equiv C[a^{2\Omega-2p} b^{2p}] = \binom{\Omega}{p} u_a^p v_a^{\Omega-p} u_b^{\Omega-p} v_b^p,$$

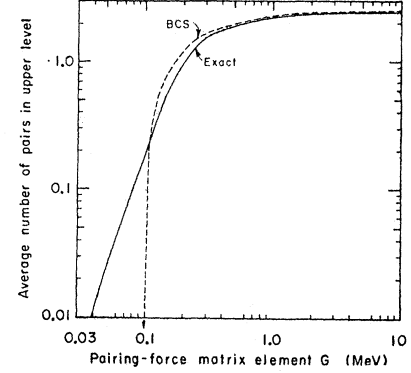


FIG. 5. Average number of pairs in the upper level $\langle \frac{1}{2}N_u \rangle$, where $j_u, j_i = 9/2$, $N = 10$, $\epsilon = 1$ MeV.

where p is number of pairs promoted from a to b . The ratio of a higher order amplitude to the lowest order one is then given by

$$\frac{C_p}{C_0} = \binom{\Omega}{p} \left(\frac{u_a v_b}{v_a u_b}\right)^p. \quad (33)$$

Substituting Eqs. (25) into Eq. (33), we finally have

$$\frac{C_p}{C_0} = \binom{\Omega}{p} \left(\frac{2G\Omega - \epsilon}{2G\Omega + \epsilon}\right)^p. \quad (34)$$

Thus, for very large pairing-force strength, the ratio approaches just $\binom{\Omega}{p}$, the number of ways of distributing p pairs in Ω places.

C. Numerical Solutions

Here we make a detailed comparison of the BCS and exact solutions for the symmetric (and the unsymmetric) example, computed over a range of pairing-force strength. The separation between the a and b levels is taken to be 1 MeV. In Figs. 5 and 6 are given the $\langle \frac{1}{2}N_u \rangle$ values versus G for the symmetric and unsymmetric cases, respectively. Notice that both cases

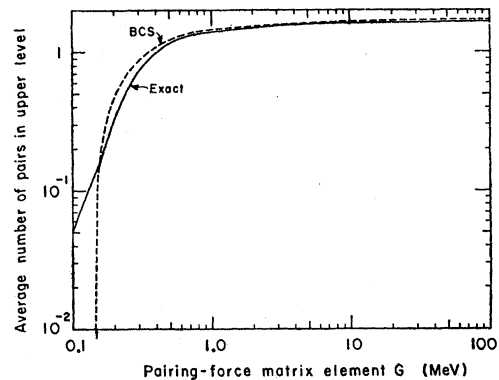


FIG. 6. Average number of pairs in the upper level $\langle \frac{1}{2}N_u \rangle$, where $j_u = \frac{3}{2}$, $j_i = \frac{7}{2}$, $N = 8$, $\epsilon = 1$ MeV.

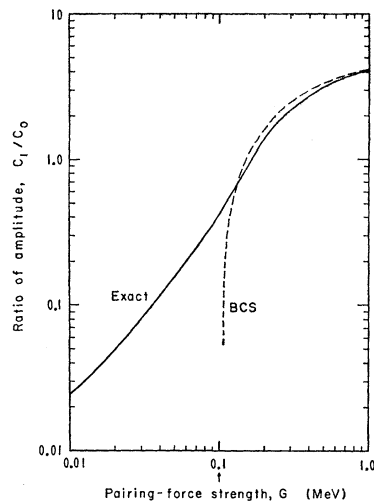


FIG. 7. The ratio of amplitudes C_1/C_0 in the symmetric case with $\Omega_u = \Omega_l = 5$, $N = 10$, $\epsilon = 1$ MeV.

exhibit a similar appearance. We shall now look more closely at the symmetric case. In this case, the critical pairing-force strength $G_c = 0.1$ MeV. The average number of pairs in the upper level $\langle \frac{1}{2} N_u \rangle$ coincides for BCS and exact solution at a force just above critical, and thereafter the BCS solution remains above the exact solution. At larger G the two methods approach asymptotically. The exact wave function here has six components and we now wish to compare BCS and exact solutions with respect to all components. In Figs. 7 through 9, are plotted the ratios of amplitudes for the symmetric, degenerate case analogous to Figs. 1 through 3. It is to be noted that there always occurs a crossover of the two ratios, and also that the largest error is made in the amplitude for promotion of a single pair, the error being smaller in the higher order components. The crossover points do not all occur at exactly the same force strength, but there is actually a region of maximum accuracy of the projected BCS wave function just above threshold.

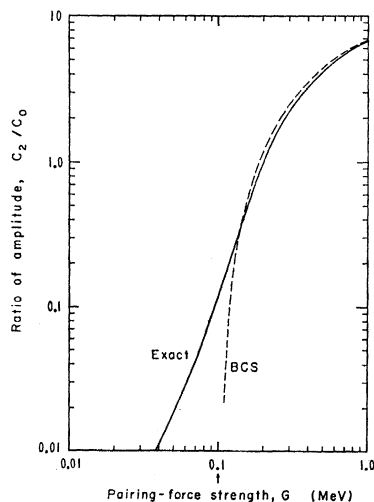


FIG. 8. The ratio of amplitude C_2/C_0 in the symmetric case with $\Omega_u = \Omega_l = 5$, $N = 10$, $\epsilon = 1$ MeV.

One other point to be noted is the existence of inflection points in the ratios of amplitudes in the exact solution. In the absence of an analytical solution for the exact case the precise force strength G where the inflection point occurs is not sharply determined; however, it appears to occur very close to G_c , that is, just where the configuration mixing ceases to be present in the BCS method. The configuration mixing in the exact solution drops rapidly at G_c ; however, whereas the BCS solution goes down all the way to zero, there always remains configuration mixing of the pair-promotion type in the more correct solution. Thus, the breakdown of the BCS method at G_c is probably an exaggerated manifestation of such a change of configuration mixing. The sharp transition between superfluid and normal states of nuclear matter is clearly an artificial feature of the BCS approximation, for the size of our system is comparable to those in real nuclei.

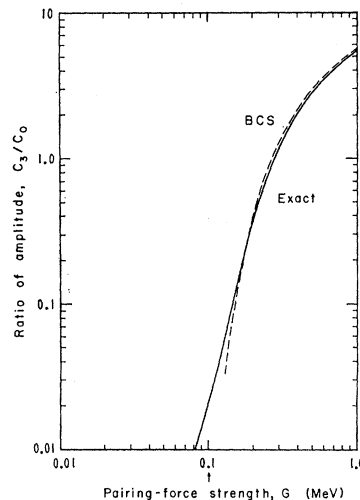


FIG. 9. The ratio of amplitude C_3/C_0 in the symmetric case with $\Omega_u = \Omega_l = 5$, $N = 10$, $\epsilon = 1$ MeV.

It is important to keep in mind two distinct types of error associated with BCS solutions. The first arises from the presence of wave function components with spurious numbers of particles, and projecting out the spurious components from a BCS solution, we see, results in a considerable decrease in error above critical force strength. The remaining error is associated with the spurious phenomenon of the sharp superfluid-normal phase transition. The projected BCS solution simply has fewer variational parameters than the degrees of freedom in the system. Further marked improvements without an increase in the number of variational parameters have been achieved by Dietrich, Mang, and Pradal⁹ through performing the variation with the fixed-particle Hamiltonian expression, rather than first solving the BCS equations. Also Mikhailov¹⁰ has achieved improved solutions by inserting renormal-

¹⁰ I. N. Mikhailov, Zh. Eksperim. i Teor. Fiz. 45, 1102 (1963) [English transl.: Soviet Phys.—JETP 18, 761 (1964)]. J. Bang and I. N. Mikhailov, P-1573, Joint Institute for Nuclear Research, Dubna, 1964 (to be published).

ized G_{eff} and ϵ_{α} values into the BCS equations. Both these methods give nontrivial solutions, no matter how weak the pairing-force strength. Such new methods appear to be of great importance in pairing-force calculations where small or no configuration mixing would appear in the ordinary BCS solutions.

ACKNOWLEDGMENTS

We are grateful to Dr. Hans J. Mang for helpful discussions and to J. K. Poggenburg for providing some numerical results for comparison here.

This work was done under the auspices of the U. S. Atomic Energy Commission.

New Isotope $\text{In}^{124}\dagger$

M. KARRAS*

Department of Chemistry, University of Arkansas, Fayetteville, Arkansas

(Received 27 January 1964; revised manuscript received 27 April 1964)

Irradiation of Sn^{124} samples with 14–15-MeV neutrons was found to produce a new radioactive nuclide which was assigned to In^{124} . The following radiation characteristics have been observed to belong to the decay of In^{124} : half-life, 3.6 ± 1.0 sec; beta end-point energy, 5.3 ± 0.8 MeV; gamma rays having energies 1.13 ± 0.01 MeV, 0.99 ± 0.02 MeV, and 3.21 ± 0.03 MeV, and relative intensities 100, 33 ± 7 , and 33 ± 7 , respectively.

THE investigation of In^{124} has been a continuation of recent work on indium isomers of mass numbers 118, 120, and 122, in connection with the systematic study of energy levels in the even tin isotopes.¹ The indium isomers were produced in (n, p) reactions in various samples of enriched tin isotopes, by irradiating them with 14–15-MeV neutrons from the neutron generator at the University of Arkansas. The same procedure was apparently favorable in the case of In^{124} , too. Because the activation cross section of the (n, p) reaction in Sn^{124} turned out to be several times smaller than that of the reaction $\text{Sn}^{122} (n, p) \text{In}^{122}$, a sample containing 300 mg of 96% enriched metallic Sn^{124} was needed (supplied by Stable Isotopes Division, Oak Ridge National Laboratory, Oak Ridge, Tennessee). In order to obtain satisfactory statistics, the pulse-height spectra had to be accumulated from several hundred short runs. Typically, some 1000 counts were collected to the gamma-ray peaks of the new activity in the spectra, the background not being higher than that within the peak. The stability of the electronics was carefully checked and the shift in calibration amounted to less than 1% during every experiment.

The detectors used in the investigation were two 3×3 -in. NaI(Tl) crystals and one $1\frac{1}{2}$ -in. diameter, 1-in. deep plastic beta detector. A fast pneumatic transport system was available to bring samples to the detection room. For details of irradiation and detection techniques used, see Ref. 2.

None of the radiations from other indium isomers previously detected after short irradiations of enriched samples of Sn^{118} , Sn^{120} , and Sn^{122} were observed from the fast transport Sn^{124} capsule, chemically identical and bombarded under the same conditions. This supports the fact that the 3.6-sec activity is a neutron-induced reaction product of Sn^{124} . The dominating activities in the Sn^{124} sample were N^{16} from contaminating oxygen and a 40-min Sn^{123} as a ($n, 2n$) product of Sn^{124} .

In the decay of In^{124} , as in the decay of every indium isomer studied earlier, the first excited 2^+ state of the product nucleus could be expected to be populated at least in part of the disintegrations. The first excited state of Sn^{124} is well known to lie at 1.13 MeV,³ and as anticipated a gamma ray of energy 1.13 ± 0.01 MeV was observed in the singles gamma spectrum of the irradiated Sn^{124} sample, exhibiting a much more rapid decay than N^{16} . Two other gamma rays of energies 0.99 ± 0.02 MeV and 3.21 ± 0.03 MeV were found to follow the same decay rate as the 1.13-MeV gamma. The relative intensities of the 0.99 and 3.21-MeV gammas were measured to be $33 \pm 7\%$ of the intensity of the 1.13-MeV gamma. The result, 3.6 ± 1.0 sec, for the half-life was obtained by following the decay of the photopeaks of the three gammas in many consecutive spectra.

The beta spectrum was badly masked by the strong betas from N^{16} , but by comparing the spectrum of the Sn^{124} sample with the pure N^{16} spectrum, a short-lived excess of about 10% was found in the former. The half-life of the fast decaying part of the spectrum was found to agree within the limits of error with the gamma half-life. The beta spectrum had the main component with

[†] Work supported by the U. S. Atomic Energy Commission Contracts AT-(40-1)-277 and AT-(40-1)-1313.

* Present address: Institute of Physics, University of Oulu, Oulu, Finland.

¹ J. Kantele and M. Karras (to be published).

² J. Kantele and M. Karras, Phys. Rev. **129**, 270 (1963).

³ B. L. Cohen and R. E. Price, Phys. Rev. **123**, 283 (1961).